



Article

# Strain-Relief Patterns and Kagome Lattice in Self-Assembled C<sub>60</sub> Thin Films Grown on Cd(0001)

Zilong Wang, Minlong Tao, Daxiao Yang , Zuo Li , Mingxia Shi, Kai Sun, Jiyong Yang and Junzhong Wang \*

School of Physical Science and Technology, Southwest University, Chongqing 400715, China; fragment@email.swu.edu.cn (Z.W.); taotaole@swu.edu.cn (M.T.); yangdx@email.swu.edu.cn (D.Y.); lizuo212@163.com (Z.L.); smx1215@email.swu.edu.cn (M.S.); skqtt@swu.edu.cn (K.S.); jyyang@swu.edu.cn (J.Y.)  
\* Correspondence: jzwangcn@swu.edu.cn

**Abstract:** We report an ultra-high vacuum low-temperature scanning tunneling microscopy (STM) study of the C<sub>60</sub> monolayer grown on Cd(0001). Individual C<sub>60</sub> molecules adsorbed on Cd(0001) may exhibit a bright or dim contrast in STM images. When deposited at low temperatures close to 100 K, C<sub>60</sub> thin films present a curved structure to release strain due to dominant molecule–substrate interactions. Moreover, edge dislocation appears when two different wavy structures encounter each other, which has seldomly been observed in molecular self-assembly. When growth temperature rose, we found two forms of symmetric kagome lattice superstructures, 2 × 2 and 4 × 4, at room temperature (RT) and 310 K, respectively. The results provide new insight into the growth behavior of C<sub>60</sub> films.

**Keywords:** STM; C<sub>60</sub>; heptamer; kagome lattice; superstructure



**Citation:** Wang, Z.; Tao, M.; Yang, D.; Li, Z.; Shi, M.; Sun, K.; Yang, J.; Wang, J. Strain-Relief Patterns and Kagome Lattice in Self-Assembled C<sub>60</sub> Thin Films Grown on Cd(0001). *Int. J. Mol. Sci.* **2021**, *22*, 6880. <https://doi.org/22136880>

Academic Editor: Alexander A. Kamnev

Received: 18 May 2021  
Accepted: 20 June 2021  
Published: 26 June 2021

**Publisher's Note:** MDPI stays neutral with regard to jurisdictional claims in published maps and institutional affiliations.



**Copyright:** © 2021 by the authors. Licensee MDPI, Basel, Switzerland. This article is an open access article distributed under the terms and conditions of the Creative Commons Attribution (CC BY) license (<https://creativecommons.org/licenses/by/4.0/>).

## 1. Introduction

The structures and growth process of C<sub>60</sub> monolayer grown on metal surfaces have attracted widespread interest in the past decades due to the unique physical and chemical properties [1–3]. In the fullerene family, C<sub>60</sub> was the first member to be created and most extensively discussed. C<sub>60</sub> molecules form various self-assembled structures when deposited on different types of substrate, such as Au [4–9], Ag [10–14], Cu [15,16], Pb [17], Pd [18], P [19], Al [20], graphene [21–24], WSe<sub>2</sub> [25], Si [26–29], and Ge [30–32]. Many results indicate that C<sub>60</sub> molecules are easy to nucleate at the terrace edge and may form a close-packed structure under appropriate conditions, regardless of the types of substrate, such as the 2√3 × 2√3 R30° domain on Au(111) [33,34] and the 4 × 4 superstructure on graphene/Cu(111) [22].

Strain plays a central role in governing the structures of self-assembled thin films when organic molecules are deposited onto solid surfaces [35–38]. Strain derives from the competition between molecule–molecule interactions and molecule–substrate interactions. Currently, several strain relaxation mechanisms are known, such as step bunching [39], faceting [40], misfit dislocations [41,42], and the formation of periodic domain boundaries [43,44], due to the dominant molecule–substrate interactions of the different layers [45]. In the STM images of the C<sub>60</sub> monolayer, the individual C<sub>60</sub> molecules appear as a bright or dim contrast [4–16]. The various arrangements of the bright and dim C<sub>60</sub> molecules combined with the multiple molecular orientations lead to the formation of a series of superstructures in the C<sub>60</sub> monolayer, such as 2 × 2 [8,25,26], 3 × 3 [5,21], √19 × √19 [28,29], 7 × 7 [4,5,9], and a triple-stripe phase [18]. Moreover, the kagome lattices built from intersecting triangles and hexagons are observed in some C<sub>60</sub> monolayers [8,13,23]. It is necessary to study the behavior of bright or dim contrast in kagome lattice when the C<sub>60</sub> thin film is under strain.

In divalent metal Cd, there is a Coulomb repulsion between the 4d electrons and conduction band electrons, which leads to electrons with strong anisotropy in the mean

free path and heat conduction. Recently, the Cd(0001) surface was shown to be a good substrate for observing and investigating strain phenomena of epitaxial films [46,47].

In this study, we used Cd(0001) thin films grown on Si(111)- $7 \times 7$  as a substrate to explore the interface structures of the C<sub>60</sub>-Cd system. The STM study demonstrated that the C<sub>60</sub> thin films on the Cd(0001) surface presented diversity at different growth temperatures. When the growth temperature was close to 100 K, an unexpected wavy structure driven by compressive strain appeared. Two lines of the molecular arrangements were curved and corresponded to the  $\sqrt{3}$  directions of the Cd(0001) surface. Moreover, an edge dislocation was observed when two neighboring wavy domains with different directions were encountered. When the growth temperature increased, two kinds of symmetric kagome lattice, superstructures ( $2 \times 2$  and  $4 \times 4$ ) were identified in the C<sub>60</sub> domains, where individual C<sub>60</sub> molecules exhibited a bright or dim contrast.

## 2. Results and Discussion

### 2.1. An Individual C<sub>60</sub> Seven-Molecule Cluster at Two Bias Voltage

When a small amount of C<sub>60</sub> molecules was deposited on the Cd(0001) surface at 100 K, they formed individual small clusters. Figure 1A shows a typical C<sub>60</sub> heptamer (seven-molecule cluster) with one central C<sub>60</sub> molecule surrounded by six peripheral molecules. At the bias of 1.2 V, except for the central molecule with a dim protrusion, the other six peripheral C<sub>60</sub> molecules revealed a similar bright contrast. When the bias was reduced to 0.5 V, the upper-right C<sub>60</sub> molecule marked by the arrow became dim and revealed a two-lobe shape (Figure 1B). We speculate that the main mechanism for the contrast changes of this molecule arises from the modification of the molecular orientation during low-bias scanning. To the best of our knowledge, such forms of isolated C<sub>60</sub> heptamers were not reported in previous experiments.

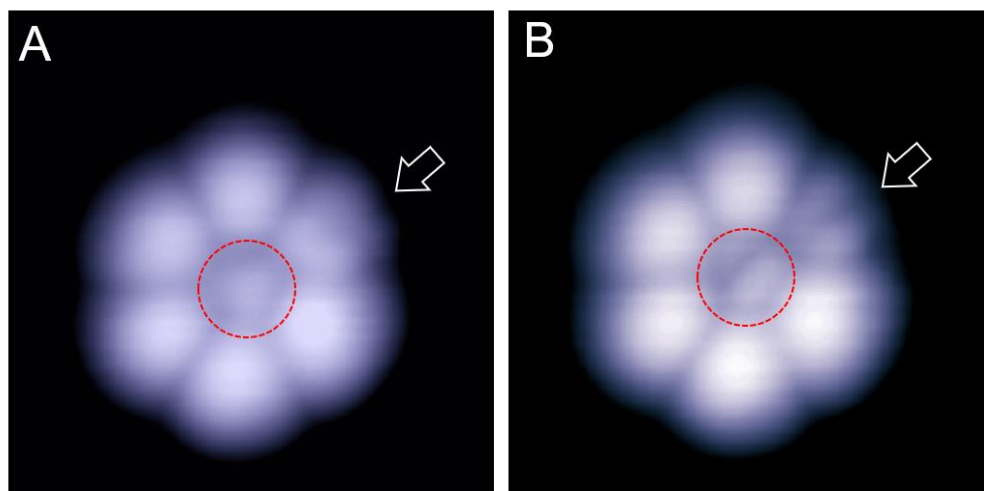


**Figure 1.** Isolated C<sub>60</sub> heptamer form on the Cd(0001) surface at 100 K. (A,B) The empty-state STM images ( $6 \times 6$  nm) recorded at 1.2 and 0.5 V, respectively. The central molecule which is marked by a red circle manifests a triangle shape at 1.2 V (A), and a two-lobe motif at 0.5 V (B). The peripheral C<sub>60</sub> molecule marked by the arrow also shows a two-lobe motif in (B).

### 2.2. Wavy Structure of the C<sub>60</sub> Submonolayer Appears at 100 K

As molecule coverage increased, an unexpected wavy structure of the C<sub>60</sub> submonolayer appeared. Figure 2A is the STM image of a wavy domain where the C<sub>60</sub> molecules in the (120) direction present a wavy arrangement while the molecules in the (110) direction are arranged in a straight line. Both directions correspond to the  $\sqrt{3}$  directions of the Cd(0001) surface. The three rows marked with red curves demonstrate the wavy arrangement clearly. Figure 2B displays another wavy domain and the direction of straight alignment has an angle of 60 degrees with respect to Figure 2A. The intermolecular spacing

is  $9.8 \pm 0.1 \text{ \AA}$  in the straight rows and  $9.4 \pm 0.1 \text{ \AA}$  in the wavy rows. Both are apparently smaller than the preferred spacing ( $10.02 \text{ \AA}$ ) of the (111) plane in fcc  $C_{60}$  crystals [48], indicating a 2% compressive strain in straight molecular rows, and a 6.3% compressive strain in wavy molecular rows.

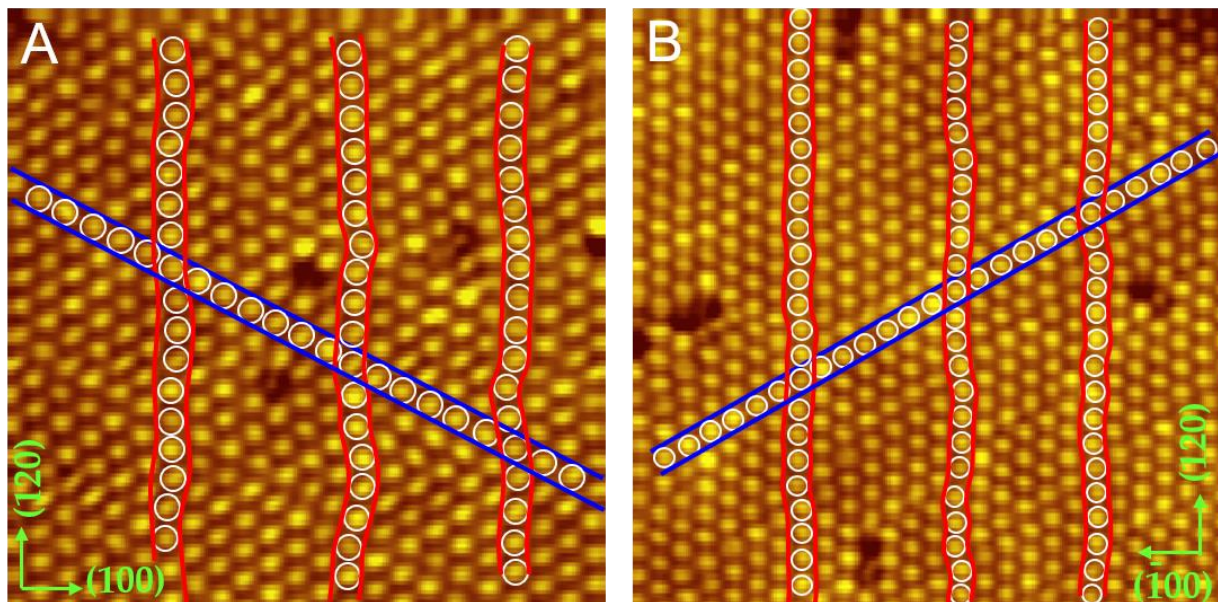


**Figure 2.** Wavy structure of the  $C_{60}$  submonolayer driven by compressive strain. **(A)** A wavy domain showing the wavy arrangement in the (120) direction, and the straight arrangement in the  $(\bar{1}10)$  directions, 0.9 V,  $20 \times 20 \text{ nm}$ . Both directions correspond to the  $\sqrt{3}$  directions of the Cd(0001) surface. **(B)** Another domain showing the wavy alignment of  $C_{60}$  molecules, 0.4 V,  $22.7 \times 22.7 \text{ nm}$ . The direction of straight alignment has an angle of 60 degrees with respect to that in **(A)**.

When  $C_{60}$  submonolayers were subjected to external forces,  $C_{60}$  molecules correspond with stable orientations to attach to the substrate. However, it was not enough to release the stress by orientation and a wavy structure appeared. Driven by the compressive stress, the individual  $C_{60}$  molecules deviated from linear arrangement, and the molecular rows became wavy in order to release the strain. In early studies, when the molecule-substrate force worked as a dominant role, slightly curved stripes were also observed in  $C_{60}$  films deposited on an Si(111)  $4 \times 1 \text{ In}$  surface [49]. In addition to unidirectional wavy structures, we observed another strain relaxation pattern through the formation of edge dislocations in the  $C_{60}$  monolayer.

### 2.3. High-Resolution Topological Graph of the Edge Dislocation

Figure 3A shows another area of the wavy structures comprising two neighboring wavy domains (I and II) with different directions for the straight alignments. The straight arrangements and wavy arrangements in Domain I and II are marked with blue curves and red lines, respectively. The straight arrangement in Domain II is in the (120) direction, while the straight arrangement in Domain I is in the (210) direction. When these domains encounter each other, an edge dislocation appears at the domain boundaries, tagged with white dotted lines. To the best of our knowledge, edge dislocation is seldomly precisely observed in molecular self-assembly. A similar phenomenon was achieved in the work of Klyachko, who found the edge dislocation in the third layer of  $C_{60}$  films grown on Ge(100) [31]. Unfortunately, the detail of the edge dislocation was hard to obtain due to the absence of a high-resolution STM diagram.

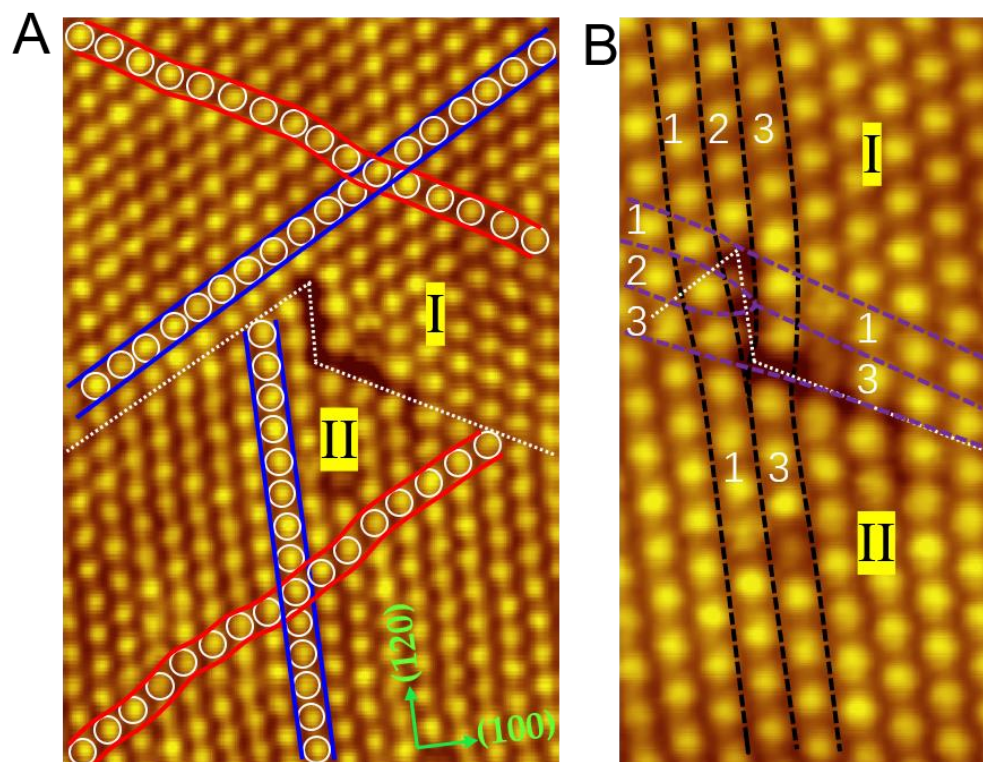


**Figure 3.** Two neighboring wavy domains (I and II) with different directions for the straight alignments. (A) Edge dislocation appears at the domain boundaries (white dotted lines),  $23 \times 15$  nm, 2.8 V. (B) Close-up view of the edge dislocation as marked by the black and purple dotted curves,  $7.5 \times 13.5$  nm, 3.0 V.

Figure 3B depicts the close-up view of the edge dislocation. Represented by black dotted lines, Domain I has an extra C<sub>60</sub> row compared to Domain II. The same situation also occurs along the purple dotted lines. This observation indicates that the edge dislocation may occur in the monolayer regime and provides an intuitive STM diagram for the study of edge dislocations. Moreover, we noticed that this type of dislocation is absent when Cd(0001) substrate is kept at RT during C<sub>60</sub> deposition.

#### 2.4. Two Regular Domains in R26° and R33°

When growth temperature is raised to RT, two types of domain appear in the C<sub>60</sub> monolayer. Figure 4A shows the topography of a R26° domain, in which all the C<sub>60</sub> molecules adopt the same orientation. Each molecule reveals a two-lobe contrast corresponding to the C<sub>60</sub> orientation with a 6:6 bond facing upward, similar to the C<sub>60</sub> molecule in Au(111) and graphene [4,22]. The molecules in this domain exhibit a hexagonal lattice constant  $a_1 = 10.0 \pm 0.1$  Å, close to the same value (10.02 Å) in C<sub>60</sub> crystals [48]. This means that there is almost no strain when C<sub>60</sub> molecules adopt the same orientation. Figure 4B shows a R33° domain that is composed of symmetric kagome lattices. Inside this domain, each dim C<sub>60</sub> molecule is surrounded by six bright molecules, constituting a head-to-head arrangement of hexagonal rings. In other words, the C<sub>60</sub> monolayer is composed of two types of molecular rows: In row-**b**, all the molecules show a bright protrusion, while in row-**a**, one bright and one dim C<sub>60</sub> molecule alternately appear. As a result, the bright and dim molecules constitute a  $2 \times 2$  superstructure, with each unit cell containing four molecules. The measured intermolecular distance is  $a_2 = 10.2 \pm 0.1$  Å, indicating a 2% tensile strain in the R33° domain. These types of symmetric kagome lattices also exist in the reported C<sub>60</sub> domains in Au(111) [8,23].

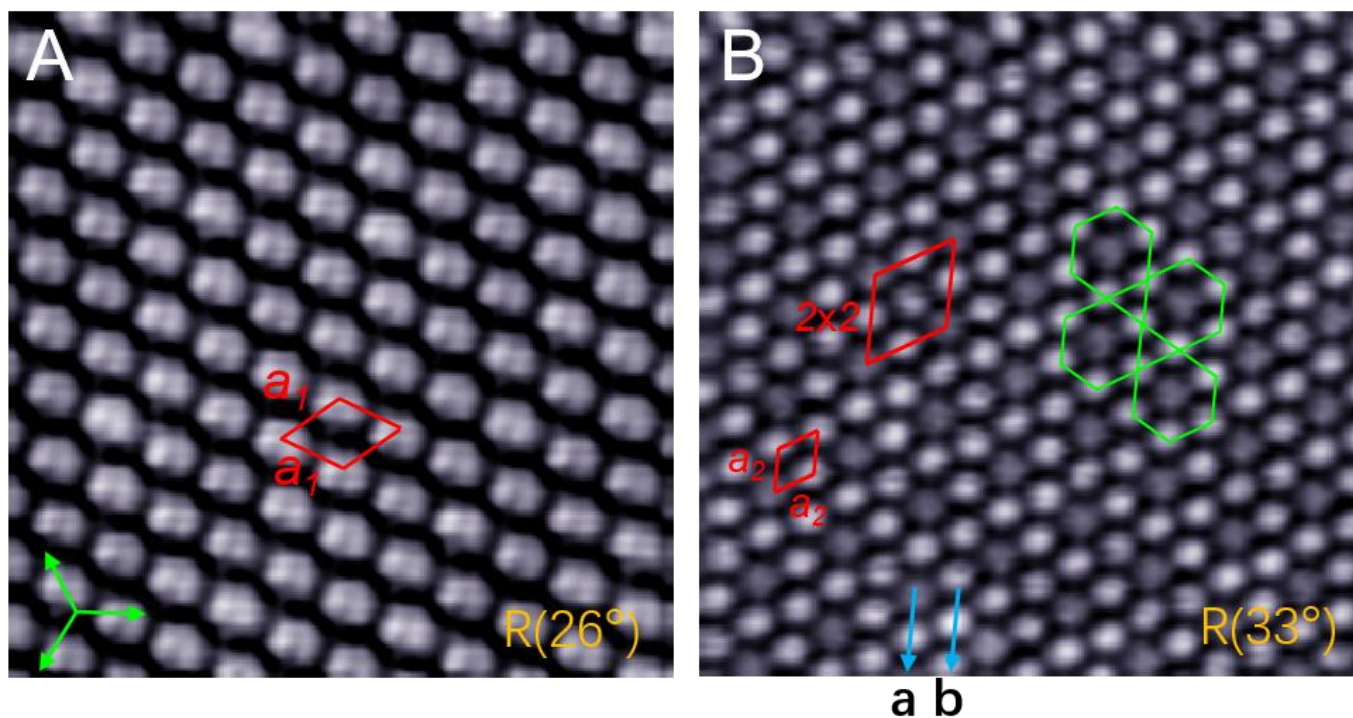


**Figure 4.** Two regular domains were obtained by deposition at room temperature. (A) Homogeneous orientation of  $C_{60}$  molecules in a  $R26^\circ$  domain, 1.2 V,  $10 \times 10$  nm. (B) The symmetric kagome lattice which is marked by hexagons in green reveals a  $2 \times 2$  superstructure in an  $R33^\circ$  domain, 2.0 V,  $15 \times 15$  nm. Arrow **b** represents the molecular rows with bright molecules, and arrow **a** represents the rows with one bright and one dim molecules alternately arranged.

#### 2.5. A larger $4 \times 4$ Superstructure of Kagome Lattice in an $R44^\circ$ Domain

When the growth temperature rises to 310 K, the  $C_{60}$  monolayer presents a larger kagome lattice with a  $4 \times 4$  superstructure, shown in Figure 5A. The intermolecular distance is  $a_3 = 10.5 \pm 0.1 \text{ \AA}$ , much larger than the value ( $10.02 \text{ \AA}$ ) in  $C_{60}$  crystals. The tensile strain is as large as 5%. These properties indicate that the packing density of  $C_{60}$  molecules decreases with an increase in growth temperature due to thermal expansion of the  $C_{60}$  layer. As displayed in Figure 5B, the six trigonal regions distribute symmetrically around the central hexagon, constituting the kagome lattice. Each kagome unit cell contains sixteen molecules: a  $C_{60}$  heptamer located at the inner hexagon and nine peripheral molecules. The heptamer consists of a central dim molecule and six bright surrounding molecules. We noticed that the  $C_{60}$  monolayer in this domain is composed of three types of molecular rows: all  $C_{60}$  molecules in row-a show a dim contrast; two dim molecules and two bright molecules are alternately arranged in row-b; one bright and one dim molecule appear alternately in row-c.

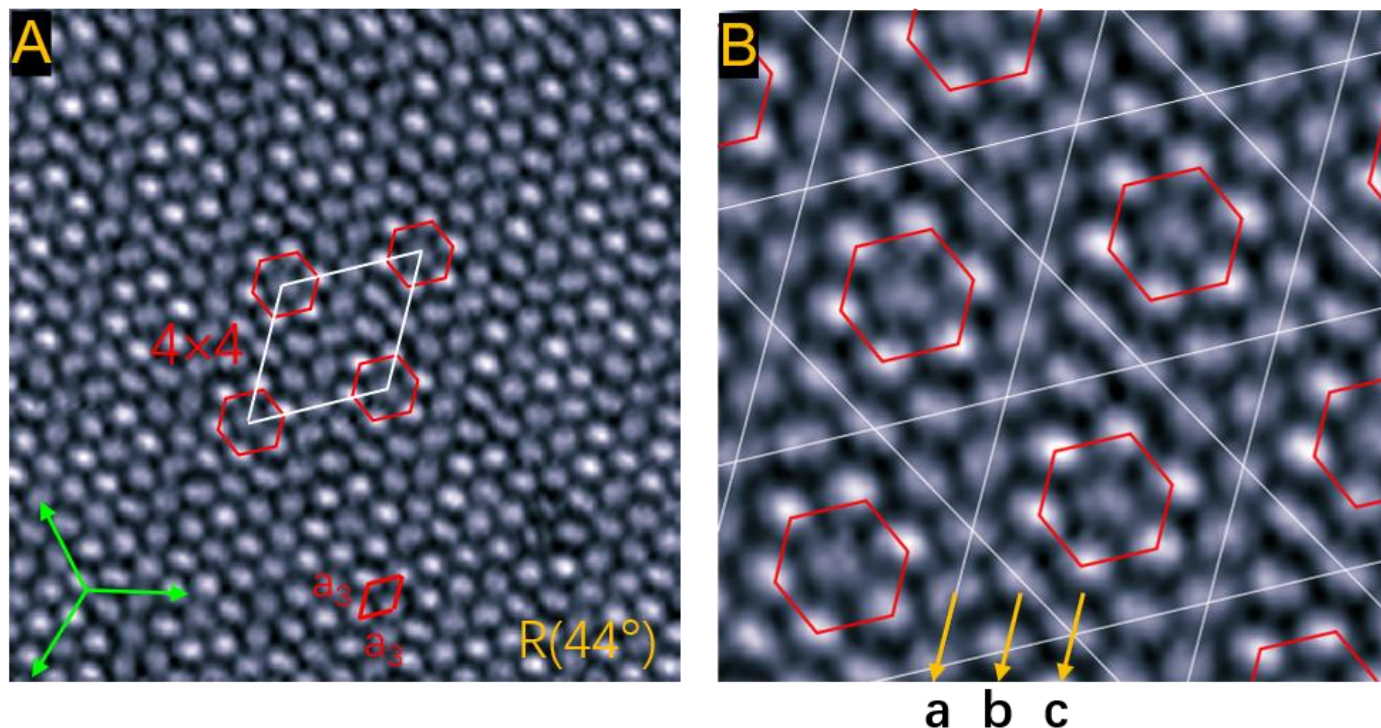


**Figure 5.** Kagome lattice formed at 310 K. **(A)** Symmetric kagome networks reveal a  $4 \times 4$  superstructure in an  $R44^\circ$  domain. The rhombus shows the primitive cell of the superstructure.  $20 \times 20$  nm, 1.2 V. **(B)** Close-up view of the kagome network with each unit cell containing sixteen  $C_{60}$  molecules, 1.2 V,  $10 \times 10$  nm. The molecular rows **a**, **b**, and **c** contain dim molecules, alternate two bright and two dim molecules, alternate one bright and one dim molecule, respectively.

### 3. Materials and Methods

The experiments were performed in an ultra-high vacuum low-temperature scanning tunneling microscopy (Unisoku, Japan) with a base pressure close to  $1.5 \times 10^{-10}$  Torr. A clean surface of Si(111)- $7 \times 7$  was obtained through thermal flashing to 1550 K after uninterrupted degassing at 820 K for more than 7 hours. The flat and smooth Cd(0001) thin film was treated by depositing 15–20 monolayers onto the surface of Si- $7 \times 7$ .  $C_{60}$  molecules were evaporated from a homemade Tantalum boat at a rate of 0.4 ML/min onto the Cd(0001) thin films. After the process was completed,  $C_{60}/Cd/Si$  was transferred into the STM observation chamber. The entire data were obtained in a constant current mode at 78 K (liquid nitrogen temperature).

### 4. Conclusions

In summary, our research showed the morphology of  $C_{60}$  molecules on Cd(0001) substrate in three different growth temperatures (100 K, RT, and 310 K). STM studies demonstrated that  $C_{60}$  molecules are bright or dim in the thin film. At 100 K, we found the isolated  $C_{60}$  seven-molecule cluster, which indicates that the  $C_{60}$  heptamer can exist alone. As the molecule coverage increased, an unexpected wavy structure appeared, which suggests the  $C_{60}$  submonolayer was subjected to a large compressive strain. As a normal reaction, when under large external stress, the film of atoms or molecules may present larger bulk density or form superstructures. In this study, the arrangement of  $C_{60}$  curved instead of the aforementioned action. Additionally, an edge dislocation was captured when two different wavy structures encountered each other, which may develop a new phenomenon to study edge dislocation. Two types of symmetric kagome lattices were found at elevated growth temperatures, the  $2 \times 2$  superstructure in the  $R33^\circ$  domain with a 2% tensile strain at RT, and the  $4 \times 4$  superstructure in the  $R44^\circ$  domain with a 5%

tensile strain at 310 K. Our results provide a new routine to fabricate and investigate pressure-resistant materials.

**Author Contributions:** J.W. designed the experiments; Z.W., D.Y. and M.S. performed the experiments; Z.W., K.S. and J.W. wrote the manuscript; M.T., Z.L. and J.Y. revised the manuscript. All authors have read and agreed to the published version of the manuscript.

**Funding:** This work was supported by the National Natural Science Foundation of China (grant Nos. 11874304, 11574253, 11604269, 11674323, and 11804282) and the Fundamental Research Funds for the Central Universities (XDJK2020B054).

**Institutional Review Board Statement:** Not applicable.

**Informed Consent Statement:** Not applicable.

**Data Availability Statement:** The data presented in this study are available on request from the corresponding author.

**Conflicts of Interest:** The authors declare no conflict of interest.

## References

1. Wachowiak, A.; Yamachika, R.; Khoo, K.H.; Wang, Y.; Grobis, M.; Lee, D.H.; Louie, S.G.; Crommie, M.F. Visualization of the molecular jahn-teller effect in an insulating  $K_4C_{60}$  monolayer. *Science* **2005**, *310*, 468–470. [[CrossRef](#)] [[PubMed](#)]
2. Feng, M.; Zhao, J.; Petek, H. Atomlike, Hollow-core-bound molecular orbitals of  $C_{60}$ . *Science* **2008**, *320*, 359–362. [[CrossRef](#)] [[PubMed](#)]
3. Mitrano, M.; Cantaluppi, A.; Nicoletti, D.; Kaiser, S.; Perucchi, A.; Lupi, S.; Pietro, P.D.; Pontiroli, D.; Riccò, M.; Clark, S.R.; et al. Possible light-induced superconductivity in  $K_3C_{60}$  at high temperature. *Nature* **2016**, *530*, 461–464. [[CrossRef](#)]
4. Schull, G.; Berndt, R. Orientationally ordered ( $7 \times 7$ ) superstructure of  $C_{60}$  on Au(111). *Phys. Rev. Lett.* **2007**, *99*, 226105. [[CrossRef](#)] [[PubMed](#)]
5. Gardener, J.A.; Briggs, G.A.D.; Castell, M.R. Scanning tunneling microscopy studies of  $C_{60}$  monolayers on Au(111). *Phys. Rev. B* **2009**, *80*, 235434. [[CrossRef](#)]
6. Wang, Y.Y.; Yamachika, R.; Wachowiak, A.; Grobis, M.; Khoo, K.H.; Lee, D.H.; Louie, S.G.; Crommie, M.F. Novel Orientational Ordering and Reentrant Metallicity in  $K_xC_{60}$  Monolayers for  $3 \leq x \leq 5$ . *Phys. Rev. Lett.* **2007**, *99*, 086402. [[CrossRef](#)]
7. Tang, L.; Xie, Y.C.; Guo, Q.M. Complex orientational ordering of  $C_{60}$  molecules on Au(111). *J. Chem. Phys.* **2011**, *135*, 114702. [[CrossRef](#)]
8. Tang, L.; Guo, Q.M. Orientational ordering of the second layer of  $C_{60}$  molecules on Au(111). *Phys. Chem. Chem. Phys.* **2012**, *14*, 3323–3328. [[CrossRef](#)] [[PubMed](#)]
9. Shin, H.; Schwarze, A.; Diehl, R.D.; Pussi, K.; Colombier, A.; Gaudry, E.; Ledieu, J.; McGuirk, G.M.; Serkovic, L.L.N.; Fournée, V.; et al. Structure and dynamics of  $C_{60}$  molecules on Au(111). *Phys. Rev. B* **2014**, *89*, 245428. [[CrossRef](#)]
10. Grobis, M.; Lu, X.; Crommie, M.F. Local electronic properties of a molecular monolayer:  $C_{60}$  on Ag(001). *Phys. Rev. B* **2002**, *66*, 161408. [[CrossRef](#)]
11. Pai, W.W.; Hsu, C.L. Ordering of an incommensurate molecular layer with adsorbate-induced reconstruction:  $C_{60}/Ag(100)$ . *Phys. Rev. B* **2003**, *68*, 121403. [[CrossRef](#)]
12. Hsu, C.L.; Pai, W.W. Aperiodic incommensurate phase of a  $C_{60}$  monolayer on Ag(100). *Phys. Rev. B* **2003**, *68*, 245414. [[CrossRef](#)]
13. Pai, W.W.; Hsu, C.L.; Lin, K.C.; Sin, L.Y.; Tang, T.B. Characterization and control of molecular ordering on adsorbate-induced reconstructed surfaces. *Appl. Surf. Sci.* **2005**, *241*, 194–198. [[CrossRef](#)]
14. Grobis, M.; Yamachika, R.; Wachowiak, A.; Lu, X.H.; Crommie, M.F. Phase separation and charge transfer in a K-doped  $C_{60}$  monolayer on Ag(001). *Phys. Rev. B* **2007**, *80*, 073410. [[CrossRef](#)]
15. Abel, M.; Dmitriev, A.; Fasel, R.; Lin, N.; Barth, J.V.; Kern, K. Scanning tunneling microscopy and x-ray photoelectron diffraction investigation of  $C_{60}$  films on Cu(100). *Phys. Rev. B* **2003**, *67*, 245407. [[CrossRef](#)]
16. Wong, S.S.; Pai, W.W.; Chen, C.H.; Lin, M.T. Coverage-dependent adsorption superstructure transition of  $C_{60}/Cu(001)$ . *Phys. Rev. B* **2010**, *82*, 125442. [[CrossRef](#)]
17. Li, H.I.; Franke, K.J.; Pascual, J.I.; Bruch, L.W.; Diehl, R.D. Origin of Moiré structures in  $C_{60}$  on Pb(111) and their effect on molecular energy levels. *Phys. Rev. B* **2009**, *80*, 085415. [[CrossRef](#)]
18. Weckesser, J.; Cepek, C.; Fasel, R.; Barth, J.V.; Baumberger, F.; Greber, T.; Kern, K. Binding and ordering of  $C_{60}$  on Pd(110): Investigations at the local and mesoscopic scale. *J. Chem. Phys.* **2001**, *115*, 9001–9009. [[CrossRef](#)]
19. Cui, X.X.; Han, D.; Guo, H.L.; Zhou, L.W.; Qiao, J.S.; Liu, Q.; Cui, Z.H.; Li, Y.F.; Lin, C.W.; Cao, L.M.; et al. Realizing nearly-free-electron like conduction band in a molecular film through mediating intermolecular van der Waals interactions. *Nat. Commun.* **2019**, *10*, 3374. [[CrossRef](#)] [[PubMed](#)]
20. Ledieu, J.; Gaudry, E.; Weerd, M.C.D.; Gille, P.; Diehl, R.D.; Fournée, V.  $C_{60}$  superstructure and carbide formation on the Al-terminated  $Al_9Co_2(001)$  surface. *Phys. Rev. B* **2015**, *91*, 155418. [[CrossRef](#)]

21. Li, G.; Zhou, H.T.; Pan, L.D.; Zhang, Y.; Mao, J.H.; Zou, Q.; Guo, H.M.; Wang, Y.L.; Du, S.X.; Gao, H.J. Self-assembly of C<sub>60</sub> monolayer on epitaxially grown, nanostructured graphene on Ru(0001) surface. *Appl. Phys. Lett.* **2012**, *100*, 013304. [[CrossRef](#)]
22. Jung, M.; Shin, D.B.; Sohn, S.D.; Kwon, S.Y.; Park, N.J.; Shin, H.J. Atomically resolved orientational ordering of C<sub>60</sub> molecules on epitaxial graphene on Cu(111). *Nanoscale* **2014**, *6*, 11835–11840. [[CrossRef](#)] [[PubMed](#)]
23. Han, S.; Guan, M.X.; Song, C.L.; Wang, Y.L.; Ren, M.Q.; Meng, S.; Ma, X.C.; Xue, Q.K. Visualizing molecular orientational ordering and electronic structure in Cs<sub>n</sub>C<sub>60</sub> fulleride films. *Phys. Rev. B* **2020**, *101*, 085413. [[CrossRef](#)]
24. Chen, C.H.; Zheng, H.S.; Mills, A.; Heflin, J.R.; Tao, C.G. Temperature evolution of quasi-one-dimensional C<sub>60</sub> nanostructures on rippled graphene. *Sci. Rep.* **2015**, *5*, 14336. [[CrossRef](#)]
25. Santos, E.J.G.; Scullion, D.; Chu, X.S.; Li, D.O.; Guisinger, N.P.; Wang, Q.H. Rotational superstructure in van der waals heterostructure of self-assembled C<sub>60</sub> monolayer on the WSe<sub>2</sub> surface. *Nanoscale* **2017**, *9*, 13245–13256. [[CrossRef](#)]
26. Wang, H.Q.; Zeng, C.G.; Wang, B.; Hou, J.G. Orientational configurations of the C<sub>60</sub> molecules in the (2 × 2) superlattice on a solid C<sub>60</sub> (111) surface at low temperature. *Phys. Rev. B* **2001**, *63*, 085417. [[CrossRef](#)]
27. Nakaya, M.; Aono, M.; Nakayama, T. Molecular-scale size tuning of covalently bound assembly of C<sub>60</sub> molecules. *ACS Nano*. **2011**, *5*, 7830–7837. [[CrossRef](#)] [[PubMed](#)]
28. Matetskiy, A.V.; Gruznev, D.V.; Zotov, A.V.; Saranin, A.A. Modulated C<sub>60</sub> monolayers on Si(111)√3 × √3-Au reconstructions. *Phys. Rev. B* **2011**, *83*, 195421. [[CrossRef](#)]
29. Gruznev, D.V.; Matetskiy, A.V.; Bondarenko, L.V.; Utas, O.A.; Zotov, A.V.; Saranin, A.A.; Chou, J.P.; Wei, C.M.; Lai, M.Y.; Wang, Y.L. Stepwise self-assembly of C<sub>60</sub> mediated by atomic scale moiré magnifiers. *Nat. Commun.* **2013**, *4*, 1679. [[CrossRef](#)] [[PubMed](#)]
30. Xu, H.; Chen, D.M.; Creager, W.N. C<sub>60</sub>-induced reconstruction of the Ge(111) surface. *Phys. Rev. B* **1994**, *50*, 8454–8459. [[CrossRef](#)] [[PubMed](#)]
31. Klyachko, D.V.; Lopez-Castillo, J.M.; Jay-Gerin, J.P.; Chen, D.M. Stress relaxation via the displacement domain formation in films of C<sub>60</sub> on Ge(100). *Phys. Rev. B* **1999**, *60*, 9026–9036. [[CrossRef](#)]
32. Fanetti, M.; Gavioli, L.; Cepek, C.; Sancrotti, M. Orientation of C<sub>60</sub> molecules in the (3√3 × 3√3) R30° and (√13 × √13) R14° phases of C<sub>60</sub>/Ge(111) single layers. *Phys. Rev. B* **2008**, *77*, 085420. [[CrossRef](#)]
33. Torrelles, X.; Pedio, M.; Cepek, C.; Felici, R. (2√3 × 2√3) R30° induced self-assembly ordering by C<sub>60</sub> on a Au(111) surface: X-ray diffraction structure analysis. *Phys. Rev. B* **2012**, *86*, 075461. [[CrossRef](#)]
34. Passens, M.; Waser, R.; Karthaeuser, S. Enhanced fullerene-Au(111) coupling in (2√3 × 2√3) R30° superstructures with intermolecular interactions. *Beilstein J. Nanotechnol.* **2015**, *6*, 1421–1431. [[CrossRef](#)] [[PubMed](#)]
35. Thürmer, K.; Huang, R.Q.; Bartelt, N.C. Surface self-organization caused by dislocation networks. *Science* **2006**, *311*, 1272–1274. [[CrossRef](#)]
36. Lu, Y.F.; Przybylski, M.; Trushin, O.; Wang, W.H.; Barthel, J.; Granato, E.; Ying, S.C.; Nissila, T.A. Strain relief in Cu-Pd heteroepitaxy. *Phys. Rev. Lett.* **2005**, *94*, 146105. [[CrossRef](#)]
37. Hsu, P.J.; Finco, A.; Schmidt, L.; Kubetzka, A.; Bergmann, K.V.; Wiesendanger, R. Guiding spin spirals by local uniaxial strain relief. *Phys. Rev. Lett.* **2016**, *116*, 017201. [[CrossRef](#)] [[PubMed](#)]
38. Realpe, H.; Peretz, E.; Shamir, N.; Mintz, M.H.; Shneck, R.Z.; Manassen, Y. Islands as nanometric probes of strain distribution in heterogeneous surfaces. *Phys. Rev. Lett.* **2010**, *104*, 056102. [[CrossRef](#)] [[PubMed](#)]
39. Liu, F.; Tersoff, J.; Lagally, M.G. Self-organization of steps in growth of strained films on vicinal substrates. *Phys. Rev. Lett.* **1998**, *80*, 1268–1271. [[CrossRef](#)]
40. Mo, Y.W.; Savage, D.E.; Swartzentruber, B.S.; Lagally, M.G. Kinetic pathway in stranski-krastanov growth of Ge on Si(001). *Phys. Rev. Lett.* **1990**, *65*, 1020–1023. [[CrossRef](#)]
41. Mansour, K.A.; Buchsbaum, A.; Ruffieux, P.; Schmid, M.; Gröning, P.; Varga, P.; Fasel, R.; Gröning, O. Fabrication of a well-ordered nanohole array stable at room temperature. *Nano Lett.* **2008**, *8*, 2035–2040. [[CrossRef](#)]
42. Jankowski, M.; Wormeester, H.; Zandvliet, H.J.W.; Poelsema, B. Temperature dependent formation and evolution of the interfacial dislocation network of Ag/Pt (111). *Phys. Rev. B* **2014**, *89*, 235402. [[CrossRef](#)]
43. Lai, M.Y.; Wang, Y.L. Metal/semiconductor incommensurate structure with a rare domain configuration exhibiting p31m symmetry. *Phys. Rev. B* **2000**, *61*, 12608–12611. [[CrossRef](#)]
44. Zegenhagen, J.; Fontes, E.; Grey, F.; Patel, J.R. Microscopic structure, discommensurations, and tiling of Si(111)/Cu “5 × 5”. *Phys. Rev. B* **1992**, *46*, 1860–1863. [[CrossRef](#)] [[PubMed](#)]
45. Gorji, N.E.; Tanner, B.K.; Vijayaraghavan, R.K.; Danilewsky, A.N.; McNally, P.J. Nondestructive, in situ mapping of die surface displacements in encapsulated IC chip packages using x-ray diffraction imaging techniques. In Proceedings of the IEEE Electronic Components and Technology Conference, Orlando, FL, USA, 30 May–2 June 2017. [[CrossRef](#)]
46. Xie, Z.B.; Wang, Y.L.; Tao, M.L.; Sun, K.; Tu, Y.B.; Yuan, H.K.; Wang, J.Z. Ordered array of CoPc-vacancies filled with single-molecule rotors. *Appl. Surf. Sci.* **2018**, *439*, 462–467. [[CrossRef](#)]
47. Yang, D.X.; Wang, Z.L.; Shi, M.X.; Sun, K.; Tao, M.L.; Yang, J.Y.; Wang, J.Z. Orientational transition of tin phthalocyanine molecules in the self-assembled monolayer. *J. Phys. D Appl. Phys.* **2020**, *53*, 154004. [[CrossRef](#)]
48. Heiney, P.A.; Fischer, J.E.; Mcghee, A.R.; Romanow, W.J.; Denenstien, A.M.; McCauley, J.P.; Smith, A.B.; Cox, D.E. Orientational ordering transition in solid C<sub>60</sub>. *Phys. Rev. Lett.* **1991**, *66*, 2911–2914. [[CrossRef](#)]
49. Kotlyar, V.G.; Olyanich, D.A.; Utas, T.V.; Zotov, A.V.; Saranin, A.A. Self-assembly of C<sub>60</sub> fullerenes on quasi-one-dimensional Si(111)4×1-in surface. *Surf. Sci.* **2012**, *606*, 1821–1824. [[CrossRef](#)]